Chemical Physics Letters 545 (2012) 44–49

Contents lists available at SciVerse ScienceDirect

Chemical Physics Letters

journal homepage: www.elsevier.com/locate/cplett

Hydrogen trapped in Be_n cluster cages: The atomic encapsulation option

Fedor Y. Naumkin [a,*], David J. Wales [b]

[a] Faculty of Science, UOIT, Oshawa, ON L1H 7K4, Canada
[b] Department of Chemistry, University of Cambridge, Cambridge CB2 1EW, United Kingdom

ARTICLE INFO

Article history:
Received 22 May 2012
In final form 11 July 2012
Available online 20 July 2012

ABSTRACT

Core–shell (kH)@Be_n (k = 1–3, n = 6–11) systems are studied computationally. The smallest system with endohedral hydrogen is H@Be_6 with a central H anion, thermodynamically stable to dissociation into H + Be_6. Larger structures are constructed by merging a few such units and have reduced stability. Potential energy barriers to hydrogen exit from the cage assemblies are estimated. Face- and edge-sharing combinations of the structural units are considered. The extrapolated upper bound for the potential 'nanofoam' material storage capacity is 10 weight-% of hydrogen. The changes in shape and electronic properties of the Be_n cages upon insertion of hydrogen are also analyzed.

1. Introduction

Reliable storage of hydrogen with straightforward release on demand is currently the bottleneck for a hydrogen-based economy. Hydrocarbon molecules as well as bulk metal-hydride solids can provide high storage capacity, but hydrogen release requires high temperatures due to a relatively large binding energy of a few eV, far above the estimated optimal value of 0.5 eV [1]. Use of chemisorption on metal surfaces in order to weaken the hydrogen-metal bonding, via fewer neighbors, reduces the capacity, but even downsizing to clusters may fail to reduce the barrier to release sufficiently.

One promising avenue to explore involves higher-energy isomers with lower binding energies, especially species with non-covalent interactions. At the solid-state scale, this situation corresponds to physisorption on surfaces, and corresponding weakly bound structures are also found for clusters, both associated with a barrier to dissociative chemisorption of H_2. Recent examples include non-dissociative attachment of H_2 molecules to mixed/doped and pure clusters of lighter metals (providing higher storage capacity), such as M_nA_k and M_n (M=Be, Al; A=Li, Na, Mg, B, P, C, Si, etc.) [2–5]. The binding energies for such systems are, however, about 0.1 eV per molecule. The corresponding chemisorbed isomers can provide values of up to 0.7 eV per molecule, but also have desorption barriers of about 1 eV. Other possible substrates for hydrogen include metal-doped hydrocarbons (see, e.g., [6,7]) and carbon polyatomics ([8] and references therein), which may be capable of achieving the optimal binding energy.

Alternative weakly bound systems can occur when hydrogen is inserted inside light-metal (Be, Mg, Ca) cluster cages [5,9,10]. Such isomers can even be higher in energy than the separate molecule plus metal cluster, but stabilized by a low potential barrier, of about 0.5 eV for H_2@Be_{10}. The low-temperature regime required to preserve the integrity for such systems may perhaps be practically more affordable, and the release of hydrogen is downhill in energy. An additional potential advantage is a realistic scaling of the system to larger size in terms of metal nanofoams, which can be viewed as aggregated cluster cages, optimally with shared walls to increase storage capacity. The feasibility of trapping hydrogen inside such aggregates has been predicted for two merged Be_n (n = 8–10) cages [11].

Endohedral hydrogen molecules dissociate due to strong charge transfer from the surrounding metal shell, and become pairs of anions suspended electrostatically inside the cages [5,9]. Their repulsion significantly affects the stability of the system. In the present Letter we therefore consider the feasibility of atomic storage for hydrogen, with each H atom encapsulated in a smaller metal cage, and assess the preservation of such atom-filled cages in a cluster assembly. In addition, insertion of an H_2 core into a Be_n shell modifies the structure and properties [5]. Here we consider the analogous changes associated with atomic hydrogen encapsulation. Of particular interest is the possible manifestation of electronic open-shell character in properties such as the excitation, ionization and electron-attachment energies. Besides a more complete characterization of the system itself, these parameters also indicate its propensity to chemical reactions.

Earlier work focused on trapping H atoms inside B_{12} cages [12,13]. It was predicted that hydrogen would not be encapsulated, but instead escape to the cluster surface. Since even for two repelling H anions inside smaller Be_n cages such escape involves overcoming a potential barrier [5], we expect a single endohedral H atom to be further stabilized in such cages.

* Corresponding author. Fax: +1 905 7213304.
E-mail address: fedor.naumkin@uoit.ca (F.Y. Naumkin).

0009-2614/$ - see front matter © 2012 Elsevier B.V. All rights reserved.
http://dx.doi.org/10.1016/j.cplett.2012.07.027

2. Computational techniques and tools

All calculations were carried out at the MP2 level of theory with standard aug-cc-pVTZ basis sets [14], as implemented in the NWChem package of ab initio programs [15]. The accuracy of this approach for the present systems was verified previously [5] by comparing the predicted and experimental parameters for constituent diatomics.

All structures were fully optimized with no symmetry restrictions. The Be_n clusters were optimized first, and then an H atom was inserted or added externally in different geometries, followed by reoptimization. We combined some of the smaller preoptimized $H@Be_n$ systems to make larger ones, with subsequent reoptimization of the composite systems. For ionic derivatives, charges were added to the optimized neutral species, followed by relaxation. After minimization the normal mode frequencies were checked to confirm that the stationary points were local minima. Potential energy barriers for hydrogen exit from the cages were estimated by pulling H through a gap between Be atoms: an appropriate Be–H distance was fixed at a series of values and all the other coordinates were reoptimized for each displacement.

Basis set superposition errors were corrected with a standard counterpoise procedure [16]. Both the lowest and higher-spin electronic states were investigated to establish the multiplicity of the ground state, which was not the lowest possible spin in some cases. Vertical excitation, ionization and electron-attachment energies were obtained by single point calculations at the optimized geometries of the neutral ground state systems. Charge distributions were evaluated within the natural bond orbital formalism [17], which exhibits a relatively low sensitivity to the basis set.

3. Results and discussion

3.1. HBe_4

Tetrahedral Be_4 is too small to accommodate a H atom, which instead escapes to the surface, attaching centrally over a triangular face (Figure 1). Despite a significant H–Be_4 binding energy (Table 1), the beryllium cluster maintains an almost unperturbed symmetry while slightly shrinking by 0.15 Å in terms of the atom–atom separation. Electron density is donated to hydrogen (Table 2), largely from the most distant Be atom.

Another isomer, higher in energy by 0.05 eV, has H bridging two Be atoms (Figure 1). Here the symmetry is significantly disturbed, with the two beryllium atoms attached to H closest together (Table 1) and the other pair 0.1 Å further apart, with both distances shorter than in isolated Be_4. The hydrogen atom carries about the same charge as in the previous case, while the charge distribution over the Be_4 unit is reversed, with the Be atoms nearer to H being most positive, consistent with the Be–H distances being shorter than for the other isomer. Nevertheless, this isomer has a larger dipole moment (Table 2).

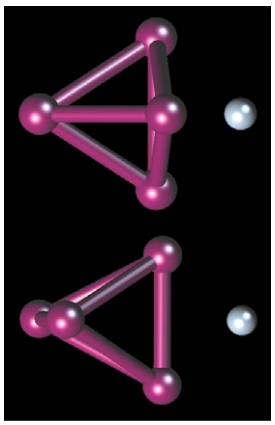

Figure 1. Optimized geometries of HBe_4 face-capped (top) and edge-bridged (bottom) isomers.

Ionization and electron attachment do not alter the shape of either isomer. The relative stability is conserved for the two cations, the first isomer becoming about 0.5 eV more stable, and switched for the anions, the second isomer becoming 0.1 eV lower in energy (Table 3).

3.2. $H@Be_6$

The Be_6 cluster is a distorted octahedron, and the smallest species that can accommodate atomic hydrogen endohedrally, transforming the cage into a symmetrical octahedron with H at its centre (Figure 2). The Be–Be distances all take a value in the middle of the range for isolated Be_6 (1.87 to 2.39 Å when calculated at the same level of theory). The H–Be_6 binding energy for this isomer is only slightly less than for HBe_4 (Table 1), and the hydrogen atom is more negative in $H@Be_6$ (Table 2), since there are more Be donors.

In contrast to $H@Be_4$, the ground electronic state of $H@Be_6$ has a higher spin value of $S = 3/2$. The $S = 1/2$ state is higher in energy by 0.3 (0.6) eV with (without) the BSSE correction. This result can be related to the charged beryllium shell having a slightly lower energy (by 0.4 eV) for the higher-spin state, which follows from additional calculations for Be_6^+ frozen in its geometry in $H@Be_6$. For the $S = 5/2$ state of $H@Be_6$ the energy is significantly higher and the hydrogen atom escapes from the cage.

HBe_6 structures with the H atom bridging an edge or attached centrally to a triangular face of Be_6 (Figure 2) have very similar energies about 1 eV lower. For both minima, especially the face-capped structure, the Be_6 cage deviates from octahedral symmetry less than for isolated Be_6 (Table 1). For the face-capped isomer, the H–Be_n binding energies for $n = 4$ and 6 bracket the value of 2.4 eV obtained for the corresponding bridge position of H on solid Be [18]. The barrier for the H atom to escape from inside the cage to its surface, i.e. $H@Be_6 \rightarrow HBe_6$, is estimated to be about 0.5 eV with a reverse barrier of about 1.5 eV.

For the face-capped isomer, the atoms farther from H are more charged, as in HBe_4, consistent with a larger dipole moment (Table 2). The edge-bridged isomer is slightly more stable. The Be atoms at the apices of the bipyramid carry small negative charges, and are therefore slightly shifted away from the H atom. As for HBe_4, the edge bridged by H is shortest, consistent with these atoms being most positive, with strong binding to the negatively charged H. The Be–H distances are generally shorter for the latter isomer. For both structures the H atom is somewhat less anionic than in $H@Be_6$, and the charge is slightly greater for the face-capped isomer, as expected from the number of Be donors in close proximity.

Upon either ionization or electron attachment, $H@Be_6$ changes into a distorted octahedron skewed along the longer and shorter edges of the base for the cation and anion, respectively (Figure 2). The distortion is larger for the anion than the cation, with the Be–H distances remaining uniform but increasing slightly. Both ions are predicted to have closed-shell ground states. In the anion, 80% of the extra charge goes to the positive beryllium shell, almost completely neutralizing it. In the cation, the shell not only gives away an electron, but also transfers an additional −0.6e to the central hydrogen atom.

Be_6^+ is a slightly distorted octahedron, generally resembling its $H@Be_6^+$ counterpart, while Be_6^- is a D_{4h} square-based bipyramid, significantly different from $H@Be_6^-$ in shape. Hence the distorted geometry of $H@Be_6$ can be attributed mainly to the beryllium shell in the cation but to the influence of the hydrogen core in the anion.

Table 1
Equilibrium parameters (in eV and Å) of H@Be_n.

System	D_e^{total}[a]/n; D_e[b]	R_e(H–H)	R_e(Be–H)	R_e(Be–Be)
Be_4H edge-attached	1.93 (1.63); 2.10 (2.01)		1.47	1.85–2.08
Face-attached	1.94 (1.64); 2.16 (2.04)		1.61	1.91–1.93
Be_4	1.40 (1.12)			2.06
H@Be_6	1.92 (1.56); 1.98 (1.72)		1.51	2.13
Be_6H edge-attached	2.11 (1.78); 3.11 (3.01)		1.46	1.92–2.15
Face-attached	2.09 (1.76); 2.98 (2.91)		1.59	1.99–2.07
Be_6	1.59 (1.28)			1.87–2.39
(2H)@Be_9	2.00 (1.62); −0.87 (−1.19)	1.68	1.50–1.72	2.14–2.43
Be_9 (face-merged)	2.09 (1.75)			2.01–2.24
(2H)@Be_{10}	2.09 (1.71); −0.36 (−0.77)	1.95	1.51–1.58	1.96–2.48
Be_{10} (edge-merged)	2.13 (1.79)			1.91–2.36
(2H)@Be_{11}	2.32 (1.94); −1.15 (−1.52)	1.71	1.51–2.01	2.01–2.24
Be_{11}	2.42 (2.08)			1.99–2.38
(3H)@Be_{11}	2.38 (1.99); 0.86 (0.41)	1.67	1.52–1.69	1.99–2.32
Be_{11} (face-merged)	2.30 (1.96)			1.95–2.33

[a] (kH)@Be_n → n Be + H/H_2/(H + H_2) for k = 1/2/3; values in brackets are BSSE-corrected.
[b] (kH)@Be_n → Be_n + H/H_2/(H + H_2) for k = 1/2/3; values in brackets are BSSE-corrected.

Table 2
Natural charge distributions (in e) and dipole moments (D) of H@Be_n.

System	q(H)	q(Be)	μ
Be_4H edge-attached	−0.68	+0.07, 0.27[a]	1.2
Face-attached	−0.70	+0.05[a], 0.54	0.33
H@Be_6	−0.95	+0.08–0.31	Nonpolar
Be_6H edge-attached	−0.78	−0.14–+ 0.39[a]	1.53
Face-attached	−0.82	+0.09[a], 0.18	2.43
(2H)@Be_9	−1.38	+0.15–0.42	0.19
(2H)@Be_{10}	−1.26	−0.08–+ 0.40	Nonpolar
(2H)@Be_{11}	−1.21	+0.11–0.35	0.34
(3H)@Be_{11}	−1.36	+0.16–0.46	Nonpolar

[a] Atoms nearest to H.

Table 3
Vertical excitation and ionization energies and electron affinities (in eV) of H@Be_n.

System	VE*	VIE	VEA
Be_4H edge-attached	1.11	6.81	2.13
Face-attached	2.58	6.34	1.95
Be_4	1.57	8.47	0.68
H@Be_6	0.58 [a]	6.91	0.97
Be_6H edge-attached	0.45 [a]	6.76	1.71
face-attached	0.37 [a]	7.06	1.87
Be_6	1.00	7.33	1.10
(2H)@Be_9	2.76	8.81	1.14
Be_9 (face-merged)	1.29	8.16	1.15
(2H)@Be_{10}	1.02	7.70	1.59
Be_{10} (edge-merged)	0.87	7.95	1.42
(2H)@Be_{11}	1.18	7.68	1.18
Be_{11}	1.81	8.78	1.02
(3H)@Be_{11}	3.09	6.88	2.90
Be_{11} (face-merged)	1.45	8.48	0.72

[a] S = 3/2 → S = 1/2.

The stability of the ions relative to dissociation into the charged Be_6 cluster plus H is about the same as for the neutral systems, i.e. 1.9 and 2.4 eV for the anion and cation, respectively.

Preliminary results show that for HBe_5 the H atom is located at the surface of the Be_5 cage, while encapsulation is possible for Be_7 to Be_9, but with a lower mass ratio for hydrogen storage compared to Be_6. These cages will be analyzed in a separate report.

3.3. (2H)@Be_9

The above results reveal significant stability for H@Be_6 with respect to escape of H, including charged states. We therefore attempted to combine these building blocks into larger systems. The hydrogen mass-ratio for H@Be_6 is less than 2 weight-%, and to increase this parameter as much as possible we consider face-sharing arrangements.

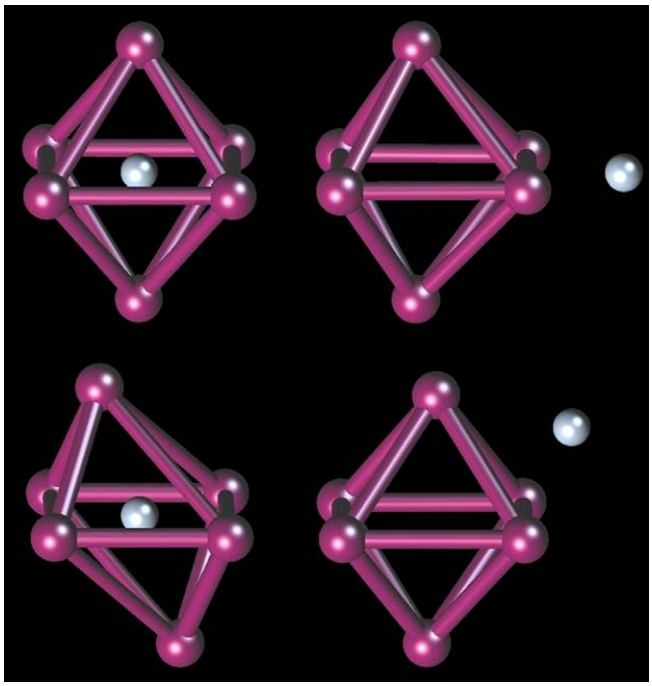

Figure 2. Optimized geometries of H@Be_6 (top left), HBe_6 edge-bridged and face-capped isomers (right), and H@Be_6^- (bottom left).

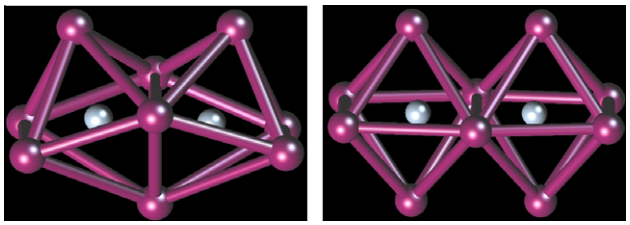

Figure 3. Optimized geometries of (2H)@Be_9 and (2H)@Be_{10} isomers constructed from two H@Be_6 units by face- and edge-sharing (left and right).

The first such system is obtained by merging triangular faces of two H@Be_6 units, which distort slightly, as shown in Figure 3. The distortion is largest away from the shared face, with increased Be–H and Be–Be distances (Table 1). The close proximity of two H anions makes the system higher in energy by about 1 eV relative to separate H_2 and a relaxed face-sharing cage. The (2H)@Be_9 system is, however, thermodynamically stable relative to separate dissociated H atoms, and is closed-shell in the ground state. The tighter encapsulation of H atoms shortens the distance between them by about 0.3 Å relative to H_2@Be_9, which is an axially capped square antiprism [5], open at the other end, making (2H)@Be_9 less stable by 2.6 eV. The H_2@Be_9 isomer is actually lower in energy than H_2 + Be_9.

The empty cage preserves its shape in the absence of hydrogen as a slightly higher energy isomer of Be_9, less than 0.1 eV above the global minimum, which is a D_{3h} tricapped trigonal prism. Insertion of H atoms stretches the cage by 0.4 Å along the H–H axis, with a corresponding compression in the perpendicular direction.

The energy barrier for one of the H atoms to exit the cage is calculated to be about 0.2 eV, lower than for H@Be_6, apparently due to the repulsion between the H anions and the distortion of the cage. For the resulting relaxed system one H caps a triangular face, and the other lies at the centre of the Be_9 tricapped trigonal prism, with an H–H@Be_9 binding energy of 3.8 eV. In contrast, detachment of recombined H_2 in such a configuration requires about 2 eV. The increased stability can be related to both the longer distance between the H anions and relaxation of the Be cage. The original (2H)@Be_9 system is stable with respect to dissociation into H + H@Be_9 by 1 eV, so the release of H_2 is energetically preferred.

Rather surprisingly, in (2H)@Be_9 each H atom carries a significantly higher negative charge than in H@Be_6 (Table 2), even though the number of Be atoms per H is smaller and the Be–H distances are longer. The overall asymmetry results in a small dipole moment.

3.4. (2H)@Be_{10}

The dopant H atoms can be spaced further apart when two H@Be_6 units share an edge (Figure 3), thus reducing repulsion between these anions. The H–H distance is then longer by about 0.3 Å compared to the above face-sharing counterpart, and while the system still has a higher energy than separate H_2 plus relaxed cage, the difference is smaller by about 0.5 eV than for the (2H)@Be_9 system (Table 1). The shared edge stretches by 0.35 Å, while the outermost ones shrink about half as much. The Be–Be distances vary more widely than for the face-sharing counterpart. The Be–H distances increase slightly and uniformly in the plane including the shared edge. Curiously, the H–H separation is then shorter than it would be (2.13 Å) for two edge-merged but unperturbed H@Be_6, apparently due to the confining cage transformation. Similar to the n = 9 case, the (2H)@Be_{10} species has a singlet ground state. However, in contrast to n = 9 the H–H distance is 0.25 Å longer than in H_2@Be_{10},which is a bicapped square antiprism [5], consistent with the latter system lying 1.0 eV above isolated H_2 and Be_{10}.

The empty cage of two edge-sharing Be_6 units behaves in a similar way, generally preserving the integrity of the building blocks. This structure is a higher-energy isomer of Be_{10}, 2.8 eV above the global minimum, with an axially bicapped square-antiprism geometry. Edge-sharing of two Be_6 units makes the Be–Be distances more even, in contrast to the situation for H@Be_6. Upon insertion of two H atoms the cage shrinks along the H–H axis by 0.2 Å and expands radially by up to 0.5 Å in the middle, the opposite of the (2H)@Be_9 case, above.

Despite having more Be neighbors and generally shorter Be–H distances, the H atoms are slightly less anionic than in (2H)@Be_9 (Table 2). This difference is consistent with the two middle beryllium atoms being negatively charged, accepting some donated electron density.

Along a pathway where one H atom exits the cage, two consecutive barriers are predicted. When the first barrier of 0.15 eV is crossed, the system transforms into a lower-energy H_2@Be_{10} isomer with an axially bicapped square-antiprism geometry [5]. The second barrier corresponds to the H atom exiting the transformed cage, and is about 0.6 eV, as found previously. Since the H_2@Be_{10} isomer is 1.9 eV lower in energy relative to (2H)@Be_{10}, the other H atom is likely to exit the cage once the initial smaller barrier is overcome.

3.5. (2H)@Be_{11}

The H anions can be further separated if two H@Be_6 units are connected in a single vertex-sharing arrangement. However, this structure was found to collapse into an equatorially bicapped Be_9 trigonal prism, with two H atoms still trapped inside (Figure 4). As a result, the H–H distance is only 0.03 Å longer than in (2H)@Be_9 (Table 1), which has an analogous structure. The Be–H distances are longer while the Be–Be separations are shorter in (2H)@Be_{11}. This difference is consistent with weaker charge transfer to the H atoms (Table 2), in spite of the larger number of Be donors. Nevertheless, the latter system has a larger dipole moment. The more compact beryllium shell thus overcomes (when collapsing) the repulsion of the more closely spaced H anions. Another possible contribution to this stabilization is the 'magic' number (20) of valence electrons in the Be_{11}^{2+} shell.

In the absence of hydrogen, the corresponding Be_{11} cage adopts a skewed version of the geometry for the hydrogenated cluster, which is longer by 0.3 Å along the H–H axis. The associated relaxation may account for the lower stability of (2H)@Be_{11} relative to H_2 + Be_{11} compared to the (2H)@Be_9 case (Table 1).

3.6. (3H)@Be_{11}

In order to see how these systems evolve with an increasing number of building blocks, another H@Be_6 was merged with (2H)@Be_9 sharing two adjacent triangular faces to produce a D_{3h}-symmetry Be_{11} cage with three hydrogen atoms trapped inside (Figure 4). The H–H and Be–H distances are almost identical (within 0.03 Å) to those for (2H)@Be_9 (Table 1), while the new system has slightly shorter Be–Be separations (by 0.1 Å). Unlike H@Be_6, the (3H)@Be_{11} system has a doublet ground state.

The empty, relaxed Be_{11} cage preserves its shape and size, with the Be–Be distances changing least among all the systems studied. The (3H)@Be_{11} species is moderately stable (Table 1) relative to isolated H_2 + H + relaxed Be_{11}. This result can be related to a

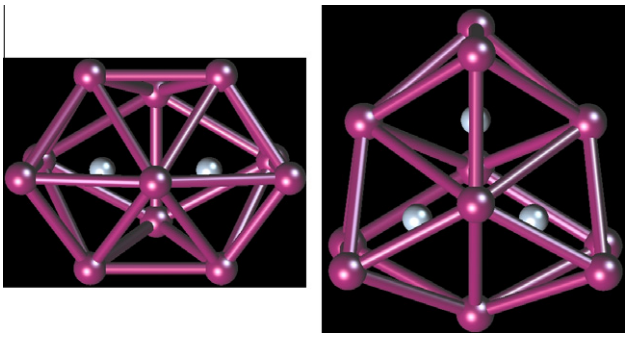

Figure 4. Optimized geometries of a (2H)@Be_{11} isomer constructed from two relaxed H@Be_6 units with a shared atom (left), and a (3H)@Be_{11} isomer constructed from three H@Be_6 with shared faces (right).

combination of the H@Be_6 unit, which is stable relative to H + Be_6, and of the metastable (2H)@Be_9 component with energy above H_2 + Be_9, consistent with the corresponding dissociation energies. When more H@Be_6 units merge, the system may thus become less stable. For example, this may happen if a fourth H@Be_6 unit is combined, due to the dissociation products $2H_2$ + Be_n recovering a second H–H bond. The (3H)@Be_{11} species is already higher in energy by about 1 eV relative to H_2 + H@Be_{11}, consistent with the (2H)@Be_9 component being destabilized by a third H anion nearby. The charges on the H and Be atoms are very similar to those for (2H)@Be_9 (Table 2), although the symmetric (3H)@Be_{11} system has no dipole moment.

Removal of a single H atom leads to a significant rearrangement of the cluster into the (2H)@Be_{11} species considered above, consistent with higher stability for the corresponding empty-cage isomer (by 1.3 eV) compared to the D_{3h} structure. The original (3H)@Be_{11} system is stable by about 0.6 eV relative to dissociation into H + (2H)@Be_{11}, which represents a competitive channel compared to products H_2 + H + $Be_{11}(D_{3h})$.

The barrier corresponding to H escape from (3H)@Be_{11} was calculated as 0.5 eV, the same as for H@Be_6, but higher than for (2H)@Be_9. This order is likely due to a lower strain energy, reflected in shorter Be–Be distances, which are on average close to those in H@Be_6, and hence a denser beryllium shell for hydrogen to pass through.

Removal of one H atom from (2H)@Be_n thus transforms the cage to its lower-energy isomers for n = 9 to 11. With all H atoms absent, the relaxed cage may preserve its shape, potentially allowing molecular hydrogen intake and recovery of the original hydrogenated species.

The anion of (3H)@Be_{11} preserves the shape of the neutral counterpart, with all atom–atom distances changing less than 0.05 Å. Ionization, however, appears to break the cluster, with an H atom escaping from the cage.

For the (kH)@Be_n systems studied here, the stability to dissociation increases monotonically with n and k. The empty cages exhibit a generally similar trend, with the exception of D_{3h} Be_{11} corresponding to (3H)@Be_{11} (Figure 5). The BSSE correction does not affect the relative stability values, instead almost uniformly reducing the dissociation energies by 0.3–0.4 eV per Be atom The clusters with two endohedral H atoms are destabilized compared to the corresponding empty cages, largely due to the recovery of the H–H bond in the dissociation products.

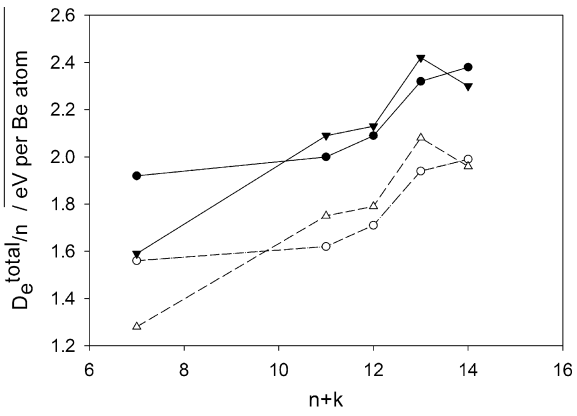

Figure 5. Total dissociation energies per Be atom of (kH)@Be_n (circles) and of the corresponding Be_n cages (shown at the same $n + k$ values) as functions of the system size, without (solid) and with (dashed) the BSSE correction.

3.7. Vertical energies

Table 3 lists the calculated vertical excitation (VE*), ionization (VIE), and electron-attachment (VEA) energies for each cluster, which should facilitate their detection in experiments. The H@Be_6 species have the lowest VE* values among all the endohedral systems, somewhat greater than for HBe_6. The highest VE*, more than fivefold larger, is found for (3H)@Be_{11}. The same clusters exhibit analogous limits for the VEA, differing by a factor of three, but with a larger VEA for HBe_6, consistent with the dipole moment of the latter species. However, the dipole moment does not appear to play a defining role for the larger systems, since (2H)@Be_{10} and (3H)@Be_{11} attract the extra electron more strongly, but have no dipoles. The VIE values are more uniform for the different clusters. As expected, they are larger for closed-shell (2H)@Be_n and peak at (2H)@Be_9 with its 'magic' 20 valence electrons. In addition, as ionization mainly involves the beryllium cage, these energies are rather insensitive to whether the H atom is inside or outside the cage, at least for H@Be_6 versus HBe_6.

Insertion of H atom(s) inside a cage can raise or lower the VE*, decreasing it for H@Be_6 and (2H)@Be_{11} and increasing it slightly for (2H)@Be_{10} and significantly for (2H)@Be_9 and (3H)@Be_{11}. The VIE values mainly decrease, except for (2H)@Be_9, which can be related to the 'magic' electron count in the latter system. The VEA values vary least, except for the fourfold increase in (3H)@Be_{11}, which might perhaps be associated with the closed shell to open-shell transition, although the same effect would operate for H@Be_6 where the VEA does not change much. The HBe_n systems with a H atom attached externally exhibit significantly increased VEA values, correlating with the dipole moment (Table 2). The vertical excitation energy for HBe_4 is significantly higher for the face-capped isomer, while the value is about the same for the two isomers of HBe_6.

4. Conclusions

A systematic ab initio investigation has been carried out for a series of beryllium cluster cages containing between one and three endohedral hydrogen atoms. The larger cages were assembled by merging Be_6 units.

The minimal such system, H@Be_6, is predicted to have O_h symmetry, with a hydrogen anion at its centre, and is thermodynamically stable with respect to dissociation into H + Be_6. It also survives electronic excitation, ionization and electron attachment, although the ions exhibit significant reversible modifications of shape, suggesting potential applications as a charge-controlled molecular switch.

The significant binding energy for a H atom inside Be_6, of about 2 eV, is expected to prevent its easy release, but is reduced in larger aggregates corresponding to H@Be_6 units merged via shared faces or edges. When empty, the larger cages preserve their shapes and correspond to higher-energy isomers of Be_n (except for n = 6). Nevertheless, with H atoms inside, they can sometimes be lower in energy relative to the separate beryllium and hydrogen components than the isomers produced from the most stable isomers of Be_n, as for (2H)@Be_{10}.

The close proximity of a few repelling endohedral H anions makes these systems significantly less stable to release of hydrogen, as for (3H)@Be_{11}, or even higher in energy than separate H_2 and Be_n, as for (2H)@$Be_{9,10}$. For the latter clusters there is a low potential energy barrier of 0.2 eV for exit of a H atom from the cage, which increases to 0.5 eV for (3H)@Be_{11}. Since the remaining H@Be_n system is stable relative to H + Be_n, the exothermic release

of H_2, recovering the H–H bond, is a more likely outcome. We hope that the present results will stimulate new experiments to investigate such effects.

From H@Be_6 to (3H)@Be_{11} the hydrogen storage capacity increases from 1.9 to 3.0 weight-%. Assuming that further units could be attached via shared faces, in the limit of space-filling H@Be_6 octahedra, with each Be atom shared by six units, we would obtain an upper bound of 10 weight-%. Even if this value is reduced by surface effects for a 'nanofoam' material, and complete recovery of hydrogen is not possible, it may still be large enough to merit further investigation. In comparison, the upper bound for larger merged H_2@Be_{10} units was estimated to be about 8 weight-% [11], this lower value being due to the lower symmetry of the Be_{10} cage and less efficient packing.

Realization of such filled-cage cluster-assembled materials might be more straightforward than macro-assemblies of clusters preserving multiple surface sites for external binding of H_2 molecules. Furthermore, production of such materials appears to be feasible already, as illustrated by experimentally created light-metal nanofoams [19] formed from elements such as Mg. As for other applications of beryllium, caution would certainly need to be exercised in any practical realization of this toxic substance for hydrogen storage.

Acknowledgements

This work was performed during the sabbatical visit of FN to the University of Cambridge. The hospitality of the Department of Chemistry is very much appreciated. The authors are also grateful for technical support from the staff of the UOIT and SHARCnet HPC facilities. Financial support of the NSERC of Canada and the RSC is acknowledged.

References

[1] J. Graetz, Chem. Soc. Rev. 38 (2009) 73.
[2] K. Srinivasu, S.K. Ghosh, R. Das, S. Giri, P.K. Chattaraj, RSC Adv. 2 (2012) 2914.
[3] L. Wang, J.J. Zhao, Z. Zhou, S.B. Zhang, Z.F. Chen, J. Comput. Chem. 30 (2009) 2509.
[4] D.J. Henry, I. Yarovsky, J. Phys. Chem. A 113 (2009) 2565.
[5] F.Y. Naumkin, D.J. Wales, Int. J. Quant. Chem. 000 (2012) 0000.
[6] E. Durgun, S. Ciraci, W. Zhou, T. Yildirim, Phys. Rev. Lett. 97 (2006) 226102.
[7] A. Chakraborty, G. Santanab, P.K. Chattaraj, Struct. Chem. 22 (2011) 823.
[8] C.-S. Liu, H. An, Z. Zeng, Phys. Chem. Chem. Phys. 13 (2011) 2323.
[9] P. McNelles, F.Y. Naumkin, Phys. Chem. Chem. Phys. 11 (2000) 2858.
[10] S. Giri, A. Chakraborty, P.K. Chattaraj, J. Mol. Model 17 (2011) 777.
[11] F.Y. Naumkin, D.J. Wales, J. Phys. Chem. A 115 (2011) 12105.
[12] R. Caputo, A. Züttel, Mol. Phys. 107 (2009) 1831.
[13] P. Wagner, C.P. Ewels, I. Suarez-Martinez, V. Guiot, S.F.J. Cox, J.S. Lord, P.R. Briddon, Phys. Rev. B 83 (2011) 024101.
[14] Basis Set Exchange, v. 1.2.2, Pacific Northwest National Laboratory, Richland, WA 99352-0999 (USA). <https://bse.pnl.gov/bse/portal>.
[15] M. Valiev et al., Comput. Phys. Commun. 181 (2010) 1477.
[16] S.F. Boys, F. Bernardi, Mol. Phys. 19 (1970) 553.
[17] A.E. Reed, L.A. Curtiss, F. Weinhold, Chem. Rev. 88 (1988) 899.
[18] A. Allouche, Phys. Rev. B 78 (2008) 085429.
[19] E.V. Skorb, D.G. Shchukin, H. Möhwald, D.V. Andreeva, Nanoscale 2 (2010) 722.